



13 March 1998

**CHEMICAL  
PHYSICS  
LETTERS**

Chemical Physics Letters 285 (1998) 59–63

## NMR spectra with peaks at the principal values of the chemical shielding tensor

Thomas M. de Swiet<sup>a,b</sup>, Marco Tomaselli<sup>a,b</sup>, Alexander Pines<sup>a,b</sup>

<sup>a</sup> *Materials Science Division, E.O. Lawrence Berkeley National Laboratory, Berkeley, CA 94720, USA*

<sup>b</sup> *Department of Chemistry, University of California, Berkeley, CA 94720, USA*

Received 16 October 1997; in final form 17 December 1997

### Abstract

The NMR chemical shielding in a solid powder sample produces featured, but broad, lineshapes, or powder patterns, because the shielding experienced by a nuclear spin depends on the spatial orientation of its local molecular frame with respect to the external magnetic field. The lineshape, however, is fully determined by the three principal values of the shielding tensor. We present a simple approach that uses sample spinning NMR to extract peaks at the principal-value frequencies from chemical shielding powder patterns. Such techniques may simplify spectra with overlapping powder patterns without the information loss inherent in fast magic angle spinning. Experimental data and numerical simulations are presented for two <sup>31</sup>P model compounds. © 1998 Elsevier Science B.V.

The chemical shielding of a nuclear spin is an orientationally dependent weighted average of the three principal values of the chemical shielding tensor (CSA) [1]. Thus in a solid powder sample each distinguishable molecular site yields an inhomogeneously broadened resonance, all possible weighted averages being present simultaneously. Under fast magic angle spinning (MAS) the time averaged chemical shielding of every crystallite in the sample reduces to the isotropic value, which is the arithmetic mean of the three principal values of the chemical shielding tensor. MAS has the advantage that unique spectral lines are often obtained for chemically distinct sites in the sample, and these lines are much more easily distinguished than the overlapping powder patterns. However, under MAS, the anisotropic information is discarded – only the average of the three principal values of the CSA tensor is measured. The three separate principal values contain not only

structural information about each individual site [1–3], but are also potentially helpful for further distinguishing different sites, since in complex materials (such as non-crystalline solids, biopolymers and solid solutions) the isotropic shifts of different sites are often more closely spaced than the residual MAS linewidth, and thus not always spectrally resolved [3] by use of the isotropic parameter alone.

The loss of anisotropic information in a MAS experiment can be partially overcome by correlating the anisotropic part of the chemical shielding interaction with the isotropic part under MAS. A variety of two-dimensional techniques have been developed to accomplish this [4–19]. The result is typically a spectrum with the isotropic shift along one frequency axis, and some form of inhomogeneously broadened powder pattern, or sideband manifold, along the second. Provided the isotropic shifts of different sites are reasonably well resolved, all three principal val-

ues of each site can be obtained by a numerical analysis of the anisotropic lineshapes.

In this Letter we demonstrate that it is possible to observe the resonance of only those spins oriented such that the rotor axis is collinear with a principal axis of the CSA. By selecting out just these three orientations, powder patterns become spectra with three peaks – one for each principal value. Potentially this makes it possible to resolve sites in a one-dimensional experiment, without loss of information about the chemical shielding tensor, although this requires spinning off the magic angle. In two dimensions one can perform isotropic/anisotropic correlation, except that in the anisotropic dimension one obtains three peaks, instead of a broad powder pattern, so that different sites with similar isotropic shifts may be resolved. In such experiments the principal values can, in principle, be simply read from the spectrum, without analysis of a powder lineshape. The limitation of such a strategy is the loss of signal to noise associated with the observation of a subset of the spins in the sample.

Under sample rotation about an axis inclined at an angle  $\theta$  to the magnetic field,  $\mathbf{B}_0$ , the chemical shielding, and thus the resonant frequency,  $\Omega_s$ , of a nuclear spin is rendered time dependent, having the following form [1] in the rotating frame

$$\Omega_s(t) = \gamma_s B_0 \left[ -1 + \sigma_{\text{iso}} + C_0 + C_1 \cos(\omega_R t + \gamma) + C_2 \cos(2\omega_R t + 2\gamma) + S_1 \sin(\omega_R t + \gamma) + S_2 \sin(2\omega_R t + 2\gamma) \right] - \omega_{r.f.} \quad (1)$$

where

$$C_0 = \frac{\delta}{4} (3\cos^2\theta - 1)(3\cos^2\beta - 1 - \eta \sin^2\beta \cos 2\alpha)$$

$$C_1 = -\frac{\delta}{4} \sin 2\theta \sin 2\beta (3 + \eta \cos 2\alpha)$$

$$C_2 = \frac{\delta}{4} \sin^2\theta (3\sin^2\beta - \eta(1 + \cos^2\beta)) \cos 2\alpha$$

$$S_1 = \frac{\delta}{2} \eta \sin 2\theta \sin \beta \sin 2\alpha$$

$$S_2 = \frac{\delta}{2} \eta \sin^2\theta \cos \beta \sin 2\alpha$$

here  $\alpha$ ,  $\beta$ , and  $\gamma$  are the Euler angles relating the principal axes of the CSA of the nuclear spin to the rotor frame [1],  $\omega_R$  is the angular velocity of the rotor,  $\gamma_s$  is the gyromagnetic ratio of the observed nuclear spin,  $S$ , and  $\omega_{r.f.}$  is the carrier frequency. The principal values of the CSA,  $\sigma_{ii}$ , have been parameterised as  $\sigma_{\text{iso}} = (\sigma_{xx} + \sigma_{yy} + \sigma_{zz})/3$  (the isotropic value),  $\delta = \sigma_{zz} - \sigma_{\text{iso}}$ , and  $\eta = (\sigma_{yy} - \sigma_{xx})/\delta$ .

The crystallite orientations that correspond to the rotor axis collinear with a principal axis of the CSA are  $\beta = \pi/2$ ,  $\alpha = 0, \pi/2$ , and  $\beta = 0$ ,  $\alpha$  undetermined. A convenient way to select these orientations is based on the fact that the zeros of  $C_1^2 + S_1^2$  occur at just these three orientations.

Under fast sample spinning the CSA contribution to the Hamiltonian may be approximated by the time average of Eq. (1),  $\bar{\sigma} = \sigma_{\text{iso}} + C_0$ . At the magic angle ( $\theta = 54.74^\circ$ ),  $C_0 = 0$ , and only the isotropic value is observed, independent of the Euler angles,  $\alpha, \beta, \gamma$ . At other angles,  $\theta$ , the spectrum is a powder pattern scaled by the term  $(3\cos^2\theta - 1)/2$ . In order to make the time dependent terms  $C_1$  and  $S_1$  take effect, they must be 'recoupled'. It is possible to use rotor synchronised radio-frequency pulses to accomplish this [4,7–9]. For the experiment described here, it is more convenient to use the rotary-resonance technique [18,20,21]. This has the advantage of ease of implementation at the expense of increased sensitivity to resonance offset.

In order to recouple the terms  $C_1$  and  $S_1$  under fast spinning, one can apply an r.f. field  $B_1$  such that the rotary-resonance condition  $-\gamma_s B_1 = \omega_{1S} = \omega_R$  is fulfilled. As discussed in [18,20,21], if one then makes a transformation to the doubly rotating frame, rotating about  $\mathbf{B}_1$  at the rotor frequency, the spins precess about a time independent field  $\mathbf{B}_{\text{eff}} = B_0 \sqrt{C_1^2 + S_1^2} / 2$  lying in the plane perpendicular to  $\mathbf{B}_1$ . The orientation of  $\mathbf{B}_{\text{eff}}$  in the perpendicular plane is determined by the third Euler angle  $\gamma$ . There are also oscillating terms which may be neglected if  $|\omega_R|$  is large compared to  $|\gamma_s B_0 \delta|$ , and any offset of the carrier frequency,  $\omega_{r.f.}$ , from  $-\gamma_s B_0 (1 - \sigma_{\text{iso}})$ .

A pulse sequence that may be used to produce spectra with contributions limited to principal-value orientations is shown in Fig. 1a. Hartmann–Hahn cross-polarisation, [22,23], is used to polarise the S

spins (e.g.  $^{13}\text{C}$ ,  $^{15}\text{N}$ ,  $^{31}\text{P}$ ,  $^{29}\text{Si}$ ), during the preparation period  $\tau_{cp}$ . During  $\tau_{rr}$ , the S spin r.f. amplitude is then matched to satisfy the rotary-resonance condition, while the I spins ( $^1\text{H}$ ) are decoupled. The S spins precess away from the  $x$ -axis with angular velocity proportional to  $B_{\text{eff}}$ . The spins in principal-value orientations have  $B_{\text{eff}} = 0$ , and so remain aligned with the  $x$ -axis. A  $(\pi/2)_y$  pulse stores the spin-locked magnetisation along the  $z$ -axis, and transverse components are quenched by turning off the I spin decoupling field during  $\tau_{zf}$ . If the cycle of rotary resonance and  $z$ -filter [24] is repeated  $N$  times, the magnetisation remaining for a given crystallite orientation is proportional to  $\cos^N(\gamma_s B_{\text{eff}} \tau_{rr})$ , which is peaked around the principal-value orientations for large  $N$ . It is noted that alternative modulations of the powder pattern may be possible with an iterative composite pulse sequence.

In order to observe spectral lines at the three distinct principal-value frequencies, the signal must be acquired with the spins evolving under the action of  $\bar{\sigma} = \sigma_{\text{iso}} + C_0$ . If the rotary-resonance filter is performed at the magic angle, then with a dynamic angle spinning (DAS) probe one option would be to hop the rotor angle to  $\theta = 0^\circ$ , and observe [19]. This

has the advantage of achieving maximum spectral separation of the principal value frequencies. Alternatively the entire experiment can be performed with a conventional MAS probe at an angle representing a compromise, in which  $C_0$  is sufficiently large for spectral separation, yet  $C_1$  and  $S_1$  are still sufficiently large that the rotary-resonance filter is efficient.

A further option is to retain the rotor at the magic angle and to perform a two-dimensional experiment (Fig. 1b). After the principle value filter, the spins evolve for a period  $t_1$  with the r.f. field satisfying the condition  $-\gamma_s B_1 = 2\omega_R$ . During the evolution period,  $t_1$ , the S spins precess about an effective field of  $B_{\text{eff}} = B_0 \sqrt{C_2^2 + S_2^2} / 2$ , and now the three principal-value crystallite orientations at which significant magnetisation remains evolve away from the  $x$ -axis at distinct frequencies. After double Fourier transformation, one obtains peaks at position  $\Omega_2 = -\gamma_s B_0 (1 - \sigma_{\text{iso}}) - \omega_{\text{r.f.}}$  in the direct dimension, and in the indirect dimension at positions  $\Omega_1 = \pm \gamma_s B_0 \delta \eta / 6$ ,  $\Omega_1 = \pm \gamma_s B_0 \delta (3 + \eta) / 12$ , and  $\Omega_1 = \pm \gamma_s B_0 \delta (3 - \eta) / 12$ .

Experiments were performed on  $^{31}\text{P}$  in two crystalline phosphates,  $(\text{NH}_4)_2\text{HPO}_4 \cdot 2\text{H}_2\text{O}$  and  $\text{CaHPO}_4 \cdot 2\text{H}_2\text{O}$ , under sample spinning at  $\theta = 40^\circ$  and at the magic angle. Results are shown in Fig. 2, together with the results of numerical simulations. The simulations are the result of integrating the time dependent Schrödinger equation for a single spin. All parameters such as r.f. field strength and spinning speed were matched to the experimental values (see the caption of Fig. 2). The effects of relaxation were not included in the simulations, but were accounted for empirically by convolution of the final spectra with a Gaussian line shape. The chemical shielding parameters ( $\delta$  and  $\eta$ ) used in the simulations were obtained from a least squares fit to the experimental powder patterns recorded at  $\theta = 40^\circ$  (Fig. 2B and F) without applying the principle value filter and under static conditions  $\omega_R = 0$  (spectra not shown). This yielded  $\delta_{\text{NH}_4} = 51 \pm 3$  ppm,  $\eta_{\text{NH}_4} = 0.35 \pm 0.04$ ,  $\delta_{\text{Ca}} = 58 \pm 3$  ppm,  $\eta_{\text{Ca}} = 0.78 \pm 0.05$ . A Gaussian homogeneous line broadening was included in the fit (full width at half height:  $\text{fwhh}_{\text{NH}_4} = 5.4 \pm 2$  ppm,  $\text{fwhh}_{\text{Ca}} = 6.4 \pm 3$  ppm), and this broadening was convolved with the simulations to produce the dashed

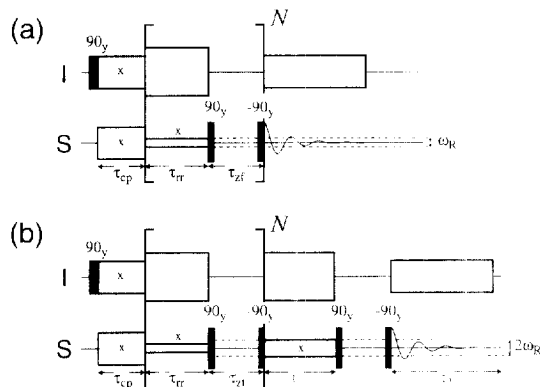


Fig. 1. One-dimensional (a) and two-dimensional (b) principal-value filter pulse sequences described in detail in the main text. In both cases Hartmann–Hahn cross-polarisation, [22,23], is used to enhance the polarisation of the S spins. The principle value orientations are selected by a series of  $N$  rotary resonance ( $\omega_{1S} = \omega_R$ ) and  $z$ -filter periods ( $\tau_{rr}$  and  $\tau_{zf}$ ). In (a) the free-induction decay can be directly detected for  $\theta \neq 54.74^\circ$ . In (b)  $\theta = 54.74^\circ$  and the selected principal-value orientations are detected indirectly by an evolution under the second rotary-resonance condition ( $\omega_{1S} = 2\omega_R$ ) during  $t_1$ .

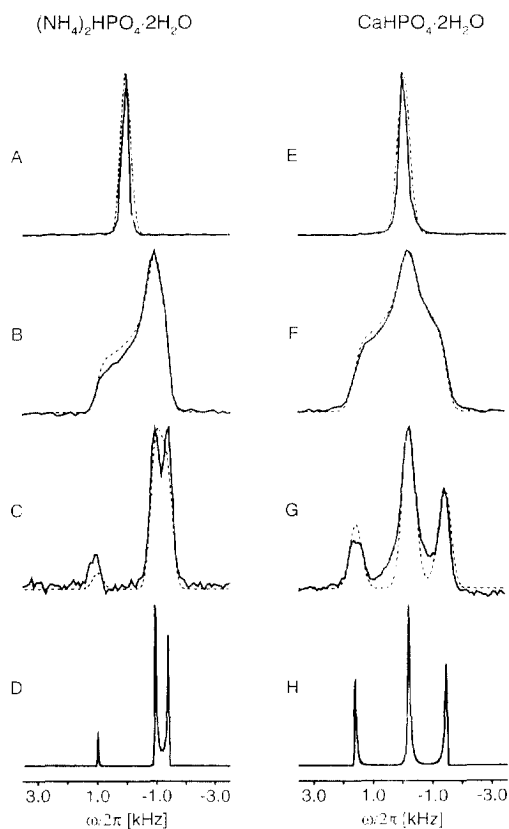


Fig. 2.  $^{31}\text{P}$  NMR spectra of crystalline powder samples of  $(\text{NH}_4)_2\text{HPO}_4 \cdot 2\text{H}_2\text{O}$ . A–D. and  $\text{CaHPO}_4 \cdot 2\text{H}_2\text{O}$ . E–H. Both compounds were purchased from Aldrich and used without further purification. The solid lines in A, E and B, F are experimental centerband spectra, after cross-polarisation from protons to  $^{31}\text{P}$ , and spinning at the magic angle and at  $\theta = 40^\circ$ , respectively. The dashed lines in B and F represent the fitted spectra as described in the text. The dashed lines in A and E show the homogeneous linebroadening used in the fits in B and F. The solid lines in C and G are experimental spectra using the pulse sequence of Fig. 1a. D and H are numerical simulations of the pulse sequence of Fig. 1a convolved with Gaussian line broadenings of 40 Hz and 48 Hz respectively. The dashed lines in C and G are the same simulations using the line broadening obtained from the fits in B and F. Spectra C–D used  $N = 33$   $\tau$ -filters, spinning at 6.6 kHz, while spectra G–H used  $N = 9$   $\tau$ -filters, spinning at 6.4 kHz. In both cases the rotary-resonance time was set to a rotor period,  $\tau_{\text{r}} = 2\pi/\omega_{\text{R}}$ , and  $\tau_{\text{rf}} = 1$  ms and  $\tau_{\text{p}} = 0.5$  ms. Experiments were performed at 300 K on a Chemagnetics Infinity spectrometer operating at 4.2 T, using a home-built MAS probe.  $90^\circ$  pulse lengths were 7  $\mu\text{s}$  on  $^{31}\text{P}$  for the pulses during  $\tau_{\text{rf}}$ .  $90^\circ$  pulse lengths on  $^1\text{H}$  were 12  $\mu\text{s}$  during decoupling and cross-polarisation.

line in plots C and G. From the experimental spectra in C and G we obtain directly values of  $\delta_{\text{NH}_4} = 49 \pm 3$  ppm,  $\eta_{\text{NH}_4} = 0.35 \pm 0.04$ ,  $\delta_{\text{Ca}} = 56 \pm 3$  ppm,

$\eta_{\text{Ca}} = 0.76 \pm 0.05$  in good agreement with the fitted values. Previously published values in the literature for these compounds are  $\delta_{\text{NH}_4} = 46$  ppm,  $\eta_{\text{NH}_4} = 0.33$ ,  $\delta_{\text{NH}_4} = 47$  ppm,  $\eta_{\text{NH}_4} = 0.5$ ,  $\delta_{\text{Ca}} = 68$  ppm,  $\eta_{\text{Ca}} = 0.6$ , [25]. Significant variations in measured values for  $\text{CaHPO}_4 \cdot 2\text{H}_2\text{O}$ , apparently reflect sample variation, for example, the amount of crystal water.

It is evident from Figs. 2D and 2H that the present technique should be capable of producing principle value spectra with small inhomogeneous linewidths. The broader linewidths observed in the experimental data are attributed to homogeneous broadening due, in part, to the  $^{31}\text{P}$ – $^{31}\text{P}$  dipolar couplings which are not averaged to zero under spinning at  $\theta = 40^\circ$ . This hypothesis is corroborated by the fact that the  $^{31}\text{P}$  linewidth under MAS is smaller than the homogeneous broadening obtained by fitting the  $\theta = 40^\circ$  spectra, as seen in Figs. 2A and 2E.

For the method described above to be effective in producing sharp principal-value spectra, it is clear that the strongest homonuclear S-spin dipole couplings must be much weaker than the width of the CSA. This condition can be satisfied for many low  $\gamma$  nuclei, such as  $^{13}\text{C}$ ,  $^{15}\text{N}$ ,  $^{31}\text{P}$ ,  $^{29}\text{Si}$ , at high external field strength  $B_0$ , using the fast spinning conditions ( $\omega_{\text{R}}/2\pi > 20$  kHz) now routinely available in commercial probes. Obviously isotopically dilute spin systems such as natural abundance, or partially enriched  $^{13}\text{C}$  are promising. Work is currently in progress in our laboratory along these lines. Using the sequence shown in Fig. 1b, we have obtained  $^{13}\text{C}$  principal-value lines in a sample of partially enriched glycine with fwhh of 2ppm in the indirect dimension. For the carboxyl site, these data yield  $\eta = 0.945 \pm 0.02$ , and  $|\delta| = 69 \pm 1.5$  ppm, in good agreement with literature values of  $\eta = 0.95$ , and  $|\delta| = 73$  ppm [2].

## Acknowledgements

The authors thank Dr. J.L. Yarger for helpful discussions. TdS is grateful for the support of the Miller Institute for Basic Research. MT acknowledges support of the Swiss National Science Foundation. This work was also supported by the Director, Office of Energy Research, Office of Basic Energy Sciences, Materials Sciences Division, U.S. Depart-

ment of Energy, under contract DE-AC03-76SF00098.

## References

- [1] M. Mehring, Principles of High-Resolution NMR in Solids, 2nd ed., Springer, Berlin, 1983.
- [2] W.S. Veeman, Prog. Nucl. Magn. Reson. Spectrosc. 16 (1984) 193.
- [3] K. Schmidt-Rohr, H.W. Spiess, Multidimensional Solid State NMR and Polymers, Academic Press, San Diego, 1994.
- [4] A. Bax, N.M. Szeverenyi, G.E. Maciel, J. Magn. Reson. 51 (1983) 400.
- [5] A. Bax, N.M. Szeverenyi, G.E. Maciel, J. Magn. Reson. 55 (1983) 494.
- [6] R.C. Zeigler, R.A. Wind, G.E. Maciel, J. Magn. Reson. 79 (1988) 299.
- [7] Y. Yarim-Agaev, P.N. Tutujian, J.S. Waugh, J. Magn. Reson. 47 (1982) 51.
- [8] R. Tycko, G. Dabbagh, P.A. Mirau, J. Magn. Reson. 85 (1989) 265.
- [9] T. Gullion, J. Magn. Reson. 85 (1989) 614.
- [10] Z. Gan, J. Am. Chem. Soc. 114 (1992) 8307.
- [11] J. Hu, D.W. Alderman, C. Ye, R.J. Pugmire, D.M. Grant, J. Magn. Reson. A 105 (1993) 82.
- [12] J.Z. Hu, W. Wang, F. Liu, M.S. Solum, D.W. Alderman, R.J. Pugmire, D.M. Grant, J. Magn. Reson. A 113 (1995) 210.
- [13] O.N. Antzutkin, S.C. Shekar, M.H. Levitt, J. Magn. Reson. A 115 (1995) 7.
- [14] A. Bax, N.M. Szeverenyi, G.E. Maciel, J. Magn. Reson. 52 (1983) 147.
- [15] J.Z. Hu, A.M. Orendt, D.W. Alderman, R.J. Pugmire, C. Ye, D.M. Grant, Solid State Nucl. Magn. Reson. 3 (1994) 181.
- [16] L. Frydman, G.C. Chingas, Y.K. Lee, P.J. Grandinetti, M.A. Eastman, G.A. Barrall, A. Pines, Isr. J. Chem. 32 (1992) 161.
- [17] L. Frydman, G.C. Chingas, Y.K. Lee, P.J. Grandinetti, M.A. Eastman, G.A. Barrall, A. Pines, J. Chem. Phys. 97 (1992) 4800.
- [18] Z. Gan, D.M. Grant, R.R. Ernst, Chem. Phys. Lett. 254 (1996) 349.
- [19] M. Tomaselli, P. Robyr, B.H. Meier, C. Grob-Pisano, R.R. Ernst, U.W. Suter, Mol. Phys. 89 (1996) 1663.
- [20] T.G. Oas, R.G. Griffin, M.H. Levitt, J. Chem. Phys. 89 (1988) 692.
- [21] M.H. Levitt, T.G. Oas, R.G. Griffin, Isr. J. Chem. 28 (1988) 271.
- [22] S.R. Hartmann, E.L. Hahn, Phys. Rev. 128 (1962) 2042.
- [23] A. Pines, M.G. Gibby, J.S. Waugh, J. Chem. Phys. 59 (1973) 569.
- [24] R.R. Ernst, G. Bodenhausen, A. Wokaun, Principles of Nuclear Magnetic Resonance in One and Two Dimensions, Clarendon Press, Oxford, 1987.
- [25] T.M. Duncan, A Compilation of Chemical Shift Anisotropies, Fargut Press, Chicago, 1990.